Chapter 16
The Effect of Chamber Temperature on Residual Stresses of FDM Parts

C. Casavola, A. Cazzato, D. Karalekas, V. Moramarco, and G. Pappalettera

Abstract The Fused Deposition Modelling (FDM) is nowadays one of the most widespread and employed processes to build complex 3D prototypes directly from a STL model. In this technique, the part is built as a layer-by-layer deposition of a feedstock wire. This typology of deposition has many advantages but it produces rapid heating and cooling cycles of the feedstock material that introduces residual stresses in the part during the building-up. Consequently, warping, de-layering and distortion of the part during the print process are common issues in FDM parts and are related to residual stresses. In the view to reduce this kind of issues, the high-level print systems use a heated chamber. The aim of the present work is to measure the residual stresses in several points of the printed parts, both on top and bottom, in order to verify if the use of the heated chamber during the printing produce substantial variation. The residual stresses have been measured in ABS parts employing the hole-drilling method. In order to avoid the local reinforcement of the strain gage, an optical technique, i.e. ESPI (electronic speckle pattern interferometry), is employed to measure the displacement of the surface due to the stress relaxation and, consequently, to calculate the residual stresses.

Keywords 3D printing · Residual stress · Fused deposition modelling · Hole drilling · ESPI

16.1 Introduction

The Fused Deposition Modelling (FDM) has become one of the most employed techniques to build prototypes and parts directly from a 3D solid model. This technology was invented in the early 1990s by Stratasys and, initially, the design verification, kinematic functionality testing and fabrication of models for visualization were the main fields where it was employed. Nowadays, there are many new fields such as aerospace, medical, construction, cultural [1, 2] and many other where it has been successfully employed. Finally, the diffusion of the low-cost desktop 3D printers such as RepRap, MakerBot, Cube, etc., has made this technology widely accessible even at home and office.

In this process, as for many others 3D printing technologies [3, 4], the model is built as a layer-by-layer deposition of a feedstock material. Initially, the raw material is in the form of a filament that is partially melted, extruded and deposited by a numerically controlled heated nozzle onto the previously built model [1]. After the deposition, the material cools, solidifies and sticks with the surrounding material. Due to the layer-by-layer construction and the orientation of the material deposition, once the entire model has been deposited, the FDM part shows orthotropic material properties with a behaviour similar to a laminate orthotropic structure [5]. Initially, the FDM printers have been able to build parts only in acrylonitrile-butadiene-styrene (ABS) and polylactic acid (PLA). However, nowadays many other materials have been employed and developed, e.g., metals [6], ceramics [7], bio-resorbable polymers (PCL) [8], metal/polymers mixture materials [9], and short fibre composites [10]. The PLA, compared to ABS, have a stronger mechanical resistance and a lower coefficient of thermal expansion. The last property improves the printability of the material because it reduces the de-layering problems and the warp effect during the printing phase. This distortion effect of the part during the printing is one of the most important issues in the FDM process, because it could seriously affect the shape and the final dimensions of the parts or it could prevent the finalization of the objects due to unsticking of the object from the bed. The distortions are due to the continuous rapid heating and cooling cycles of the deposited material [11–14]. A common and cheap technique, in order to reduce this problem, is to employ a heated bed with some type of adhesive on the surface. However, due to bad heat conduction properties of plastic

C. Casavola · A. Cazzato · V. Moramarco (✉) · G. Pappalettera
Dipartimento di Meccanica, Matematica e Management (DMMM) – Politecnico di Bari, Bari, Italy
e-mail: vincenzo.moramarco@poliba.it

D. Karalekas
Laboratory of Advanced Manufacturing Technologies and Testing, University of Piraeus, Piraeus, Greece

A. Baldi et al. (eds.), *Residual Stress, Thermomechanics & Infrared Imaging, Hybrid Techniques and Inverse Problems, Volume 7*,
Conference Proceedings of the Society for Experimental Mechanics Series, https://doi.org/10.1007/978-3-319-95074-7_16

materials, after few deposited layers the effect of the heated bed is lost. Indeed, to tackle this problem in a better way, the expensive and high-level printing systems use a heated chamber. This method, should reduce the problem related to residual stresses and distortion during the printing phase by creating a uniform temperature around the part.

Some papers have dealt with experimental measurements of residual stress distribution in plastic parts [15–17] but few works are about FDM parts [12–14]. Turnbull et al. [15] carried out a comparison among several techniques to measure residual stresses in ABS, Polycarbonate, and Nylon. They concluded that the hole drilling can be employed as a valid measurement method to measure residual stresses in plastic materials. Nau et al. [16] highlighted that the process parameters and procedures applied for stress analysis in metallic materials cannot be employed in polymers. They pointed out that the surface preparation of specimens, the strain gauge bonding, and the drilling speed are critical issues to obtain a correct measure. However, both Turnbull et al. [15] and Nau et al. [16] did not consider the local reinforcement effect that the installation of a rosette produces in materials that have a low Young's modulus. Indeed, Magnier et al. [17] studied the influence of material viscoelasticity, room temperature and local reinforcement of the strain gauge on the measure of deformation by HDM of plastic materials. They highlighted that the use of strain gauge to measure the deformation on plastic materials can produce a difference up to 30% between the results recorded by strain gauges and DIC. Casavola et al. [12–14] studied the effect on residual stresses of the raster orientation in FDM parts. They found that the stacking sequence $+45°/-45°$ shows the lowest values of residual stresses. Moreover, they showed that there is a clear effect of the constraint on the residual stress distribution highlighting that, near the edges of the parts, the residual stresses are higher. Only one paper has tried to deal with the residual stress issues in FDM part by numerical simulation. Zhang and Chou [18], using simplified material properties and boundary conditions, have simulated different deposition patterns and have demonstrated the feasibility of using the element activation function to reproduce the filament deposition. They found that there was a modification of the residual stress distributions if the tool-path pattern is changed. However, they did not validate their model using residual stress measurements but only by comparing the distortion of the printed part and the numerical prediction.

The aim of the present work is to measure the residual stresses in FDM specimens, both on top and bottom, to verify if there are any differences between a 3d printer that has a heated bed and one with the heated chamber. The residual stresses have been measured in ABS parts employing the hole-drilling method. In order to avoid the local reinforcement of the strain gage, an optical technique, i.e. ESPI (electronic speckle pattern interferometry), is employed to measure the displacement of the surface due to the stress relaxation and, consequently, to calculate the residual stresses.

16.2 Materials and Methods

A Stratasys Dimension Elite and a MakerBot Replicator 2X have been employed to produce the specimens (Fig. 16.1). The first one is a professional 3d printer with a heated chamber while the latter is a low-cost desktop 3d printer with a heated bed.

The specimens have a rectangular shape and the dimensions of $80 \times 40 \times 5$ mm with a $\pm 45°$ stacking sequences. The chosen stacking sequences was due to the limitation of the Stratasys software that does not allow modifying this parameter. Moreover, the samples have been manufactured with the minimum dimension of the part perpendicular to the build platform. The Fig. 16.2 shows the coordinate system for the residual stresses in relation to the specimen shape.

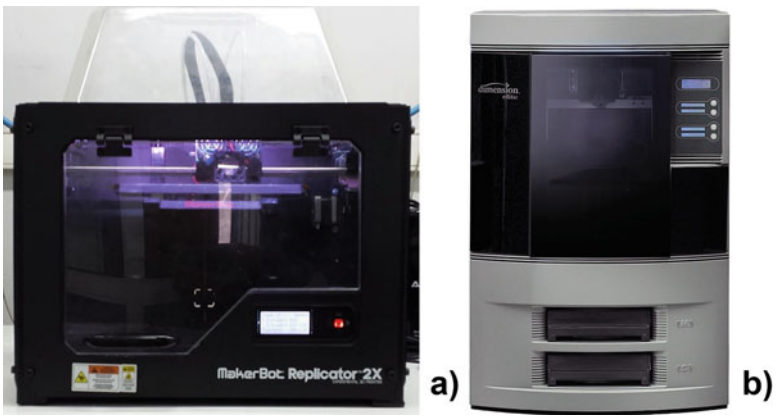

Fig. 16.1 The MakerBot 2X (**a**) and the Stratasys Dimension Elite (**b**) printers

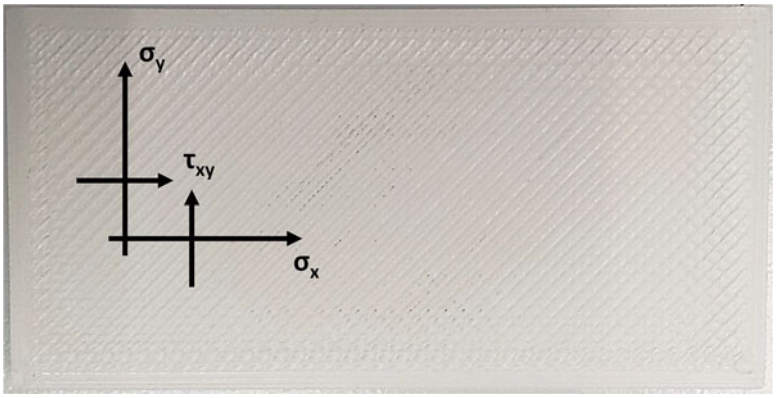

Fig. 16.2 Exemplary specimen with coordinate system for the residual stresses

Table 16.1 Fixed printer parameters

Parameter	Value
Layer thickness [mm]	0.25
Bead width [mm]	0.67
Number of contour lines	2
Bed temperature for MakerBot printer [°C]	110
Temperature of the heated chamber for Stratasys [°C]	75

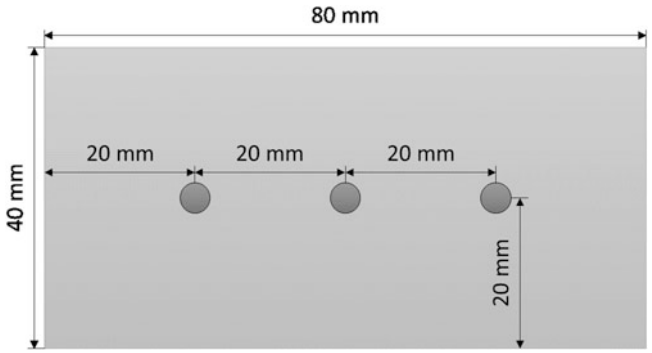

Fig. 16.3 Holes position on the top and the bottom of the specimens

The parameters reported in Table 16.1, such as the layer thickness or the number of contour lines, have been kept constant for every specimen and for each printer.

In Table 16.1, the layer thickness and the bead width are respectively the height and the width of a deposited filament. The number of contours represents how many edges have been deposited before filling the inner part by inclined beads. The solid model, created using a 3D CAD, has been sliced using the proprietary slicing software of each printer.

In this work, the ESPI technique has been employed to measure the displacement around a hole drilled inside the material. Due to the orthotropic behaviour of FDM parts, the isotropic model usually implemented in commercial hole drilling software cannot be used. Thus, an orthotropic FEM model has been developed to calculate the displacements due to some known stress cases. The combination between the experimental displacements data and the FE model allows calculating the residual stress in the parts [13].

In order to calculate the mean values of the residual stresses, the measure has been carried out on three different samples for each printer. Moreover, three holes have been drilled on the top of each specimen, i.e. starting from the last layer deposited, and three on the bottom, i.e. starting from the first layer deposited (Fig. 16.3). Finally, an average value of the three holes has been calculated and the comparison between top and bottom has been carried out.

The holes were drilled by means of a high-speed turbine which is mounted on a precision translational stage. Turbine rotation speed was set to 5000 rpm after some preliminary tests that indicated that this speed allows obtaining good quality holes [11, 19, 20]. The cutter is made by tungsten coated by TiN and it has a nominal diameter d = 1.59 mm. Compressed air was activated during the test to clean the surface of the sample by the formation of drilling chips. The holes were drilled to a depth of 0.6 mm through 12 drill increments to contain the temperature during the drilling phase at lower values.

A diode pumped solid-state laser source ($\lambda = 532$ nm) was used to shine the sample and to generate the speckle pattern. The laser beam is divided in two parts by a beamsplitter and delivered by two optical fibres. The beam emerging out from the first fibre is collimated and then directed towards the sample at a given angle ($\alpha = 53°$). The beam emerging from the second fibre, instead, is directed towards the CCD matrix of the camera and it acts as a reference beam. The CCD camera (640×480 pixel) itself is placed at a given angle with respect to the normal to the sample ($\beta = 40°$). Light diffused by the sample interferes on the CCD matrix with the reference beam. Four-step temporal phase shifting algorithm was adopted in order to obtain the phase [21, 22]. This means that four reference images are taken initially having a $\pi/2$ phase difference among each other. Another set of four images is, analogously, taken for each drill increment. These intensity patterns were subtracted from the reference intensity patterns recorded on the sample before starting the drilling procedure. This operation allows obtaining fringe patterns encoding the information about the displacement experienced by the sample along the sensitivity vector.

16.3 Results and Discussions

The σ_x, σ_y, and τ_{xy} residual stresses trends for the two printers and for the top and the bottom of the specimens have been shown in Figs. 16.4 and 16.5. As pointed out by Casavola et al. [13], the $\pm 45°$ specimens show quite low residual stresses thought higher than that reported in that work. For the τ_{xy} it cannot be observed any significant difference between the printers and, as pointed out by Casavola et al. [13], the τ_{xy} are quite low (Fig. 16.5). Indeed, the values of residual stress are roughly between -1 MPa and $+$ 1 MPa. The comparison between the MakerBot and the Stratasys residual stresses σ_x and σ_y (Fig. 16.4a, c) show that there is no clear difference on the top of the specimens. On the other hand, there are some differences, between the studied configurations, on the bottom of the specimens (Fig. 16.4b, d). These are remarkable near the surface of the specimens, i.e. until 0.2 mm, while no clear differences can be identified at higher depth [13]. The Stratasys machine, having the heated chamber, can reduce temperature difference between the deposited layer and the previous deposited material. The MakerBot printer, has only the heated bed and, due to the bad heat conduction properties

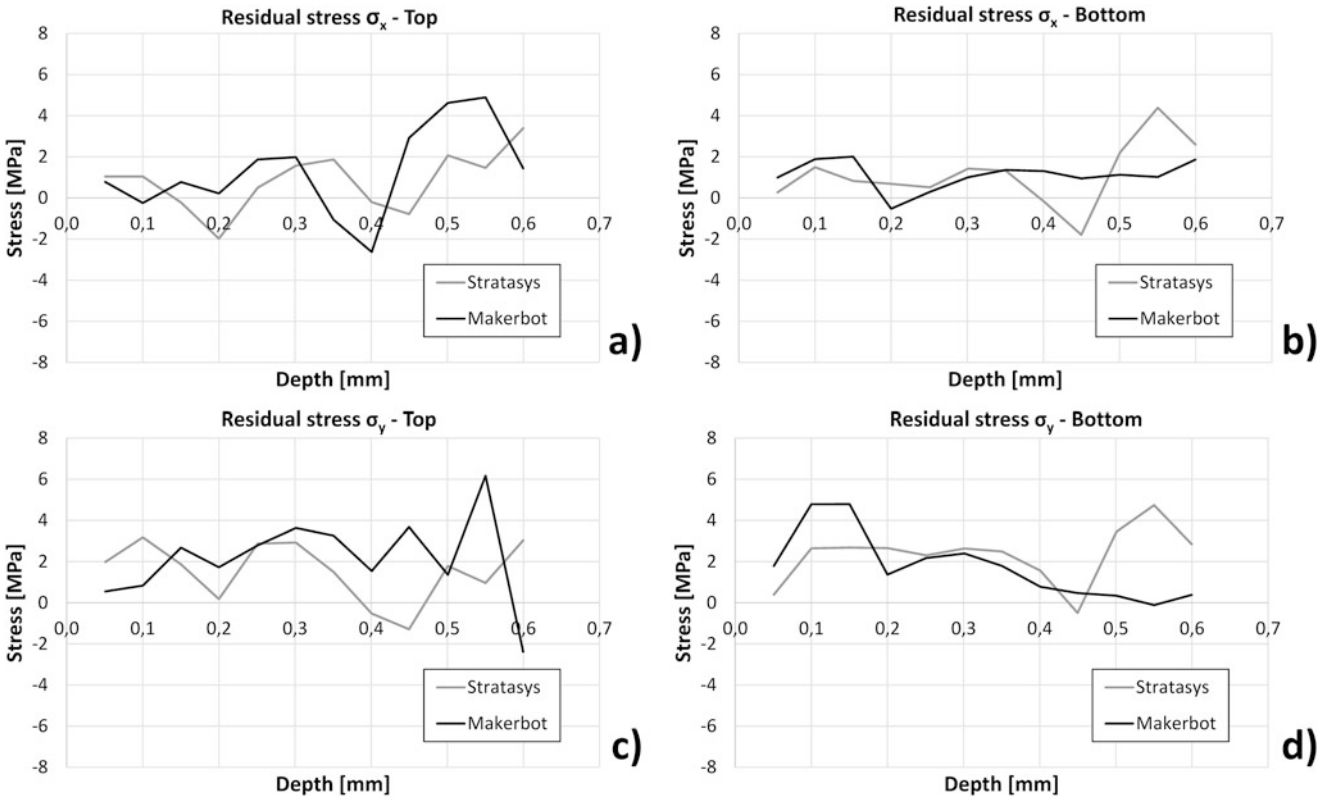

Fig. 16.4 σ_x and σ_y residual stresses for Stratasys and MakerBot printers: (**a**) σ_x top side; (**b**) σ_x bottom side; (**c**) σ_y top side; (**d**) σ_y bottom side

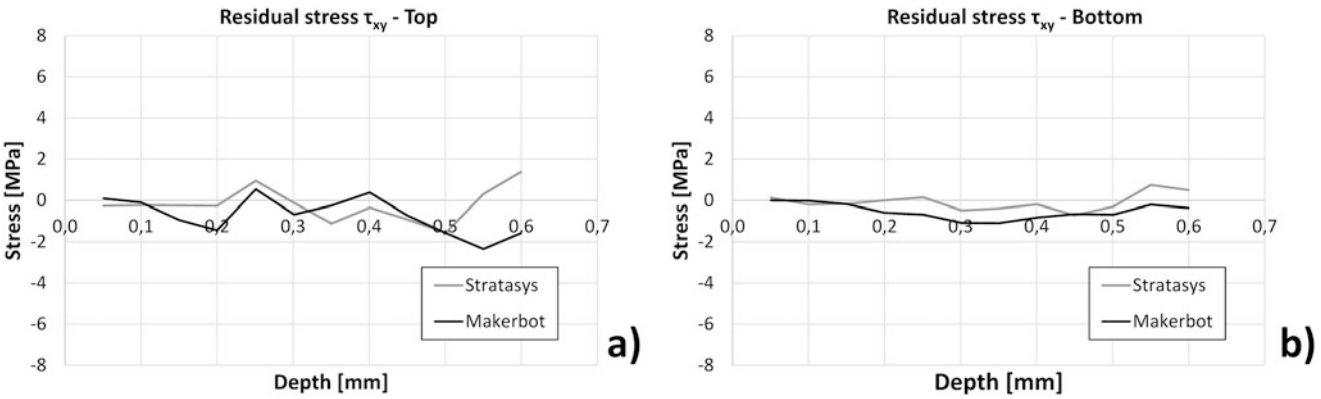

Fig. 16.5 τ_{xy} residual stresses for Stratasys and MakerBot printers: (**a**) top side; (**b**) bottom side

of plastic materials, the beneficial effect of the heated bed is reduced after few deposited layers. This can explain the higher residual stress values of the MakerBot compared to the Stratasys on the bottom of the specimens. However, it should be considered that, the MakerBot is not an open-chamber printer but it has a closed space where the hot-end prints. In this way the chamber temperature, thought is not controlled, is higher than the room temperature due to the heating effect of the bed in a closed space. In conclusion, there is a clear advantage of using a heated chamber to reduce the residual stresses in the printed parts. This difference could be clearer comparing the Stratasys machine with an open chamber machine such as RepRap in which the heat of the bed is dispersed in the room. Furthermore, we have to point out that the chosen stacking sequence ensures the lowest residual stresses, in comparison with others sequences, reducing the advantages of using heated chambers.

16.4 Conclusions

In this paper, the measure of the residual stresses in FDM printed parts has been carried out by the hole-drilling method. In order to avoid the local reinforcement of the strain gage, an optical technique, i.e. ESPI (electronic speckle pattern interferometry), is employed to measure the displacement of the surface due to the stress relaxation and, consequently, calculate the residual stresses. The aim of the work was to measure the residual stresses in several points of 3D printed parts, both on top and bottom, in order to verify if there is a clear difference between a heated bed machine and a heated chamber one. This comparison has been carried out between two printers a Stratasys Dimension Elite and a MakerBot Replicator 2X.

The results show that, whereas for σ_x and σ_y there are some differences in the bottom of the specimens, for σ_x and σ_y on the top of the specimens and τ_{xy} it cannot be observed any difference between the two printers. The differences are remarkable near the surface of the specimens, i.e. until 0.2 mm, but below this depth, there are no clear differences between the studied configurations. The Stratasys machine, having the heated chamber, can reduce temperature difference between the deposited layer and the previous deposited material and in this way the residual stress values are reduced if compared to the MakerBot. However, it should be considered that the MakerBot is not an open-chamber printer but it has a closed space where the hot-end prints. In this way the chamber temperature, thought is not controlled, is higher than the room temperature due to the heating effect of the bed in a closed space. In conclusion, there is an advantage of using a heated chamber to reduce the residual stresses in the printed parts. This difference could be clearer comparing the Stratasys machine with an open chamber machine such as RepRap in which the heat of the bed is dispersed in the room.

References

1. Yan, X., Gu, P.: A review of rapid prototyping technologies and systems. Comput. Aided Des. **28**(4), 307–318 (1996)
2. Petzold, R., Zeilhofer, H.F., Kalender, W.A.: Rapid prototyping technology in medicine—basics and applications. Comput. Med. Imaging Graph. **23**(5), 277–284 (1999)
3. Chua, C.K., Chou, S.M., Wong, T.S.: A study of the state-of-the-art rapid prototyping technologies. Int. J. Adv. Manuf. Technol. **14**(2), 146–152 (1998)

4. Barile, C., et al.: Mechanical characterization of SLM specimens with speckle interferometry and numerical optimization. Conf. Proc. Soc. Exp. Mech. Ser. **6**, 837–843 (2011)
5. Casavola, C., et al.: Orthotropic mechanical properties of fused deposition modelling parts described by classical laminate theory. Mater. Des. **90**, 453–458 (2016)
6. Mireles, J., et al.: Development of a fused deposition modeling system for low melting temperature metal alloys. J. Electron. Packag. **135**(1), 011008–011008 (2013)
7. Allahverdi, M., et al.: Processing of advanced electroceramic components by fused deposition technique. J. Eur. Ceram. Soc. **21**(10–11), 1485–1490 (2001)
8. Zein, I., et al.: Fused deposition modeling of novel scaffold architectures for tissue engineering applications. Biomaterials. **23**(4), 1169–1185 (2002)
9. Masood, S.H., Song, W.Q.: Development of new metal/polymer materials for rapid tooling using fused deposition modelling. Mater. Des. **25**(7), 587–594 (2004)
10. Zhong, W., et al.: Short fiber reinforced composites for fused deposition modeling. Mater. Sci. Eng. A. **301**(2), 125–130 (2001)
11. Kantaros, A., Karalekas, D.: Fiber Bragg grating based investigation of residual strains in ABS parts fabricated by fused deposition modeling process. Mater. Des. **50**, 44–50 (2013)
12. Casavola, C., et al.: Preliminary study on residual stress in FDM parts. In: Residual Stress, Thermomechanics & Infrared Imaging, Hybrid Techniques and Inverse Problems, vol. 9, pp. 91–96. Springer International Publishing, New York LLC (2017)
13. Casavola, C., et al.: Residual stress measurement in fused deposition modelling parts. Polym. Test. **58**, 249–255 (2017)
14. Casavola, C., et al.: Influence of printing constraints on residual stresses of FDM parts. Conf. Proc. Soc. Exp. Mech. Ser. **8**, 121–127 (2018)
15. Turnbull, A., Maxwell, A.S., Pillai, S.: Residual stress in polymers - evaluation of measurement techniques. J. Mater. Sci. **34**(3), 451–459 (1999)
16. Nau, A., et al.: Application of the hole drilling method for residual stress analyses in components made of polycarbonate. Zeitschrift Kunststofftechnik/J. Plastics Technol. **2011**(3), 66–85 (2011)
17. Magnier, A., A. Nau, B. Scholtes. Some aspects of the application of the hole drilling method on plastic materials, in Conference Proceedings of the Society for Experimental Mechanics Series, (2016)
18. Zhang, Y., Chou, Y.: Three-dimensional finite element analysis simulations of the fused deposition modelling process. Proc. Inst. Mech. Eng. B J. Eng. Manuf. **220**(10), 1663–1671 (2006)
19. Barile, C., et al.: Drilling speed effects on accuracy of HD residual stress measurements. Conf. Proc. Soc. Exp. Mech. Ser. **8**, 119–125 (2014)
20. Barile, C., et al.: Residual stress measurement by electronic speckle pattern interferometry: a study of the influence of geometrical parameters. Struct. Integrity Life. **11**(3), 177–182 (2011)
21. Kujawinska, M.: Use of phase-stepping automatic fringe analysis in moire interferometry. Appl. Opt. **26**(22), 4712–4714 (1987)
22. Ghiglia, D.C., Pritt, M.D.: Two-Dimensional Phase Unwrapping: Theory, Algorithms, and Software, vol. 4. Wiley, New York (1998)